Uncovering the Charge Transfer between Carbon Dots and Water by in situ soft X-ray Absorption Spectroscopy

*Jian Ren,[1,2] Demetra S. Achilleos,[3] Ronny Golnak,[4] Hayato Yuzawa,[5] Jie Xiao,[4] Masanari Nagasaka,[5] Erwin Reisner,[3] Tristan Petit[1]**

[1] *Institute for Nanospectroscopy, Helmholtz-Zentrum Berlin für Materialien und Energie GmbH (HZB), Albert-Einstein-Straße 15, 12489 Berlin, Germany*

[2] *Department of Physics, Freie Universität Berlin, Arnimallee 14, 14195 Berlin, Germany*

[3] *Christian Doppler Laboratory for Sustainable SynGas Chemistry, Department of Chemistry, University of Cambridge, Lensfield Road, Cambridge CB2 1EW, UK*

[4] *Department of Highly Sensitive X-ray Spectroscopy, Helmholtz-Zentrum Berlin für Materialien und Energie GmbH (HZB), Albert-Einstein-Straße 15, 12489 Berlin, Germany*

[5] *Institute for Molecular Science, Myodaiji, Okazaki 444-8585, Japan*

**E-mail: tristan.petit@helmholtz-berlin.de*

KEYWORDS. carbon dots, X-ray absorption spectroscopy, in situ characterization, solid–liquid interface, photocatalysis

ABSTRACT. Carbon dots (CDs) exhibit outstanding physiochemical properties which render them excellent materials for various applications, often occurring in an aqueous environment, such as energy harvesting and fluorescence bioimaging. Here we characterized the electronic structures of carbon dots and water molecules in aqueous dispersions using in situ X-ray absorption spectroscopy. Three types of carbon dots with different core structures (amorphous vs. graphitic) and compositions (undoped vs. nitrogen-doped) were investigated. Depending on the CD core structure, different ionic currents generated upon X-ray irradiation of the CD dispersions at the carbon K-edge were detected, which are interpreted in terms of different charge transfer to the surrounding solvent molecules. The hydrogen bonding networks of water molecules upon interaction with the different CDs were also probed at the oxygen K-edge. Both core graphitization and nitrogen doping were found to endow the CDs with enhanced electron transfer and hydrogen bonding capabilities with the surrounding water molecules.

Table of content graphics:

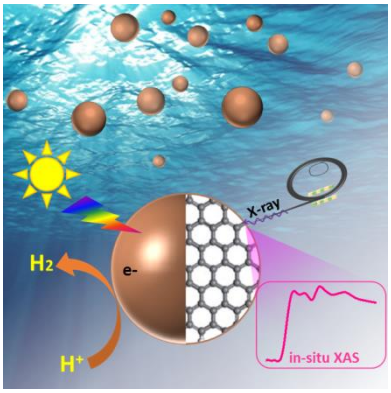

Artificial photosynthesis represents a promising approach towards clean and sustainable energy production.[1,2] Significant progress has been made in the development of novel photocatalytic materials over the last few decades. An essential feature influencing the activity of a photocatalytic material is the nature of the solid-liquid interface where transfer of the photogenerated charges occurs to drive the targeted chemical reactions. The electronic and chemical properties of this interface also govern the selectivity, rate, and overpotential of redox reactions on the photocatalyst surface.[3] However, the lack of identification of surface active sites at the atomic level limits the possibility to rationally improve performance of currently available photocatalysts.

Carbon dots (CDs) produced from "bottom-up" synthesis are of low-cost, (photo)chemically stable and have recently shown great potential as photoabsorbers in artificial photosynthesis.[4] In addition, their abundant surface active centers are favorable for high-selectivity catalytic reactions which can be effectively tuned by adjusting elemental compositions and surface functionalities.[4–6] We have recently reported a facile method to prepare scalable graphitic CDs, with (*g*-N-CD) and without (*g*-CD) core nitrogen doping as light harvester for photocatalytic hydrogen evolution reaction.[7] A significant improvement of the photocatalytic performance has been realized using *g*-N-CD due to enhanced light absorption compared to amorphous CDs (*a*-CD) and higher extraction of photogenerated charges compared to the undoped *g*-CD.[7] However, the direct spectroscopic characterization of the CD-water interface has not yet been reported. Identifying active sites leading to efficient charge transfer at the CDs surface is fundamental to facilitate the design of more effective CDs photosensitizers.

To this aim, X-ray absorption spectroscopy (XAS) is a method of interest that probes unoccupied electronic states of investigated materials, since the absorption of photons results in the

excitation of a core electron to an unoccupied state in the vicinity of the Fermi level following the dipole selection rules. XAS is an element-specific spectroscopic method, because the binding energies of core electrons vary significantly among atomic species.[8] XAS has been successfully applied ex situ on CDs powder to provide detailed information on the local chemical and electronic structures of the excited atoms.[9] On the other hand, in situ characterization in water would be necessary to assess the influence of the surrounding aqueous environment on the electronic structure of CDs. Studying the electronic structure of liquid environment and aqueous dispersion of nanomaterials under in situ condition using soft X-ray spectroscopies has attracted substantial attention in recent years.[10–12] However, a major experimental challenge is the apparent contradiction between the generally high vapor pressure of the liquid, especially water, and the vacuum requirement imposed by the short mean free path of photons in the soft X-ray range at ambient conditions. Over the years, various innovative flow cell technologies[13–16] using membranes to isolate the liquid phase from the vacuum have been devised to enable XAS measurement of liquid samples and nanoparticle dispersions.

Experimentally, the true X-ray absorption cross-section of liquid samples can be measured in the transmission mode by detecting the incoming and transmitted light through the liquid sample.[14] On the other hand, core holes are created in the X-ray absorption process and excited electrons would subsequently decay through multiple possible channels such as fluorescence and Auger decay, which enables the detection of fluorescence yield (FY) and electron yield (EY) to record the X-ray absorption (XA) spectra. The FY mode XAS measurements always suffers from low emission probabilities (< 1%) compared to the EY detection for light elements such as carbon, nitrogen and oxygen. However, the short inelastic mean-free path of emitted photoelectrons (< 10 nm) hinders their penetration through the conventional Si_3N_4 (or SiC) membranes of the

liquid cells and restricts the EY detection mainly on solid sample measurement. Recently, we have proposed an alternative detection scheme for XAS measurements to determine the total ion yield (TIY), in which the current induced by ionic species generated upon X-ray irradiation was detected.[15,17] TIY-XAS measurements have been demonstrated to be bulk-sensitive and are currently in development to characterize pure solvent and ions.[15,17–19]

In this work, the electronic structure of three CDs samples (*a*-CD, *g*-CD and *g*-N-CD) was characterized by XAS measured in total electron yield (TEY) on dry CDs in vacuum as well as transmission and TIY on CDs dispersed in water at the carbon K-edge. (Figure 1). The comparison between TEY, transmission and TIY measurements provides new insights into the carbon sites involved in charge transfer at the CDs-water interface. Furthermore, the hydrogen bonding environment of water molecules can be probed by transmission-XAS at the oxygen K-edge as previously demonstrated in pure water,[20,21] aqueous solutions[22,23] and colloidal dispersions[24,25]. The O K-edge XA spectra of the CDs dispersions at various concentrations were compared to characterize the hydrogen bonding network around CDs. By correlating the spectroscopic results to the photocatalytic performance of these CDs which have been previously studied,[7] we propose that in situ XAS could be used to investigate charge transfer properties of photocatalytic materials directly in solution.

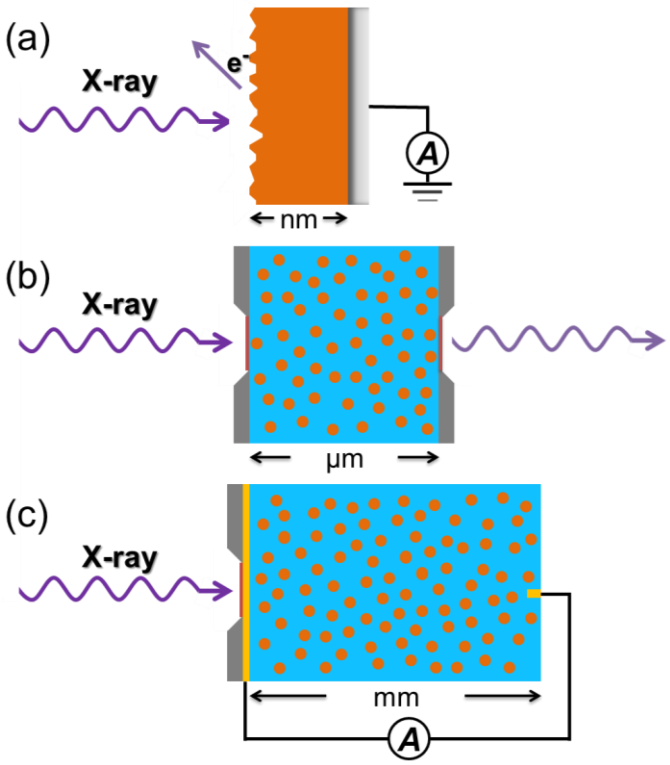

Figure 1. Schematic illustration of different XAS detection schemes: (a) TEY detection on solid materials in vacuum; (b) pure transmission and (c) TIY detection in aqueous CDs dispersion.

The XA spectra of the three CDs samples at the C K-edge are first compared (Figure 2). The TEY-XA spectra of solid samples and the transmission-XA spectra of liquid samples show similar electronic signatures. There are two sharp peaks (285.2 eV and 288.5 eV) with additional features of lower intensities in between. The pre-edge region of the TEY mode XA spectra were deconvoluted as shown in Figure 2 to better estimate the energy of the various features observed. An inverse tangent background was used to take into account the photoionization potential at the carbon K-edge (Table S1 and Figure S1).

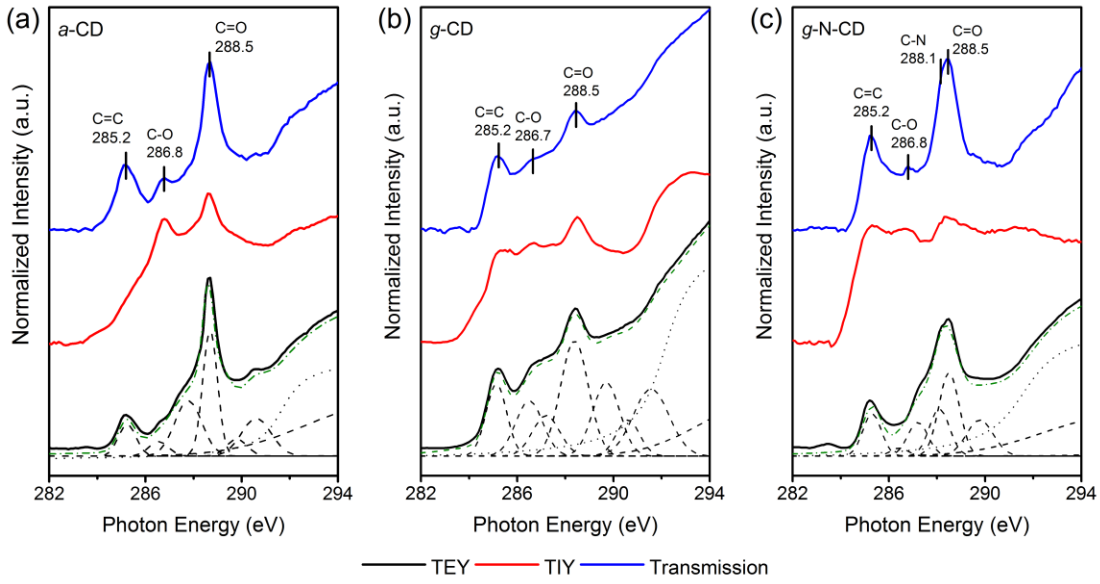

Figure 2. TEY-XA spectra (black) on dry CDs in vacuum, TIY- (red) and transmission-XA spectra (blue) in aqueous CDs dispersions at the C K-edge of (a) *a*-CD, (b) *g*-CD and (c) *g*-N-CD. The deconvoluted peaks of the TEY-XA spectra are also plotted. Different Gaussian peaks (dash), the resulting fit (green dash dot) and the background (dot) are shown below the experimental spectra. The spectra are normalized for clarity.

The feature at 285.2 eV can be unequivocally assigned to the excitation of core electrons into $\pi^*_{C=C}$ orbitals.[9] The intensity of this feature is used to estimate the percentage of the C=C contribution in *a*-CD is lower than that of the other two graphitic CDs samples. The content of the samples in sp^2 carbon is associated with their degree of graphitization, and as such confirms that the *g*-CD and *g*-N-CD are more graphitic than the *a*-CD,[26] which is in line with the respective Raman spectra of these samples.[7]

A significant change of the C=C peak intensity is observed in the TIY-XA spectra compared to TEY- and transmission-XA spectra. On TIY-XA spectrum of *a*-CD, a very weak C=C signal, which might be obscured by the tail of the nearby C−O feature, is detected (Figure 2a). However, unlike *a*-CD, the C=C feature is clearly distinguishable on TIY-XA spectra of graphitized

samples (Figure 2b,c). We interpret the different signature of *a*-CD as a result of the nature of the detected signal in TIY-XAS and the different core structure of *a*-CD compared to the graphitic samples.

Since the energy needed to excite carbon atoms (> 284 eV) is below the energy required to excite oxygen in water molecules (> 534 eV), the selective X-ray excitation of CDs is possible and the solvent is not directly ionized during in situ XAS measurements at the carbon K edge. When the carbon atoms in dispersed CDs are excited by the incident X-ray, an efficient charge separation in the CDs and a charge transfer to water molecules is required to induce an ionic current that can be detected between the two electrodes of the flow cell. For TEY-XAS, the principle is similar except that the photoelectrons are emitted in vacuum and not in liquid. The TEY-XAS of *a*-CD is close to the transmission-XAS as observed in Figure 2, showing that the photoemission yield of the *a*-CD is comparable to the graphitic CDs. The reduced TIY signal at 285 eV while $\pi^*_{C=C}$ states are available in *a*-CD, as determined by in situ transmission XAS, must therefore come from a low charge transfer efficiency of photoelectrons at the CD-water interface.

The sensitivity of XAS to short-range ordering in the material (a few atoms),[8] makes the C=C signature of *a*-CD clearly visible in transmission XAS, as for graphitic samples. However, while the C=C bonds in *g*-CD and *g*-N-CD are mostly found in ordered graphitic planes as demonstrated by XRD and HRTEM,[7,27] sp^2-hybridized carbon atoms are mainly observed in small islands isolated into an amorphous carbon matrix in the core of the *a*-CD.[27] As a result, the efficient electron transport properties of graphitic materials are not observed for *a*-CD. Electron scattering in the amorphous core may slightly reduce their kinetic energy and eventually quench the emission of photoelectron in water. As such, the above results suggest that graphitic CDs possess better charge transfer to the water molecules than the amorphous CDs. This observation

is in agreement with their more efficient electron transfer to molecular catalysts in aqueous homogenous dispersion previously reported for photocatalytic H_2 evolution.[7,27]

The features in the range between 286 and 288 eV can be assigned to the $\pi^*_{C–C–O}$ transitions in oxygen-containing groups,[9,28] whose intensities showed significant changes in the in situ TIY-XA spectra compared with the TEY-XA spectra obtained in the solid state. The shoulder at 535.5 eV for the O 1s $\rightarrow \pi^*_{C–OH}$ of the carboxyl groups[9] observed for CDs samples in the TEY-XA spectra at O K-edge (Figure S2) suggesting that the C–O features mainly originates from carboxyl groups. The sharp peak at 288.5 eV is assigned to the C 1s $\rightarrow \pi^*_{C=O}$ transitions of the carboxyl groups,[9,26] which is also supported by infrared spectroscopy[7] and the TEY-XA spectra at O K-edge (Figure S2).

The shift and broadening of the peak at 288.5 eV observed in *g*-N-CD (Figure 2c) is attributed to the additional contribution of C-N bonds (288.1 eV) close to the C=O feature (288.5 eV). In agreement, a predominant pyridinic contribution was detected at 399.7 eV in the nitrogen K-edge XA spectrum (Figure S3).[9] Another contribution in the N K-edge spectra centered at 401.7 eV may correspond to the quaternary N incorporated in six-fold aromatic cycles, including pyrimidine. These results confirmed the successful nitrogen incorporation in the core of *g*-N-CD. Nitrogen doping has a great influence on the electronic structure of carbon nanomaterials. Previous reports have confirmed that a localized density of states appears in the occupied region near the Fermi level of the carbon atoms adjacent to pyridinic nitrogen atoms, and thus suggests that carbon nanostructures containing pyridinic N possess Lewis basicity,[29–31] which is beneficial for the photoreduction of water to hydrogen.[32]

The oxygen K-edge spectra of three different CDs dispersions were subsequently compared to pure water using transmission mode XAS (Figure 3a), which is directly sensitive to the oxygen X-ray cross-section. Typical water XA spectra consist of a pre-edge at 534.7 eV, a main edge around 537 eV and a post-edge at 540 eV.[20] The overall X-ray absorption is higher for CDs dispersions than pure water but also differs with the samples. The intensity of the pre-edge feature of *a*-CD is as high as that of *g*-N-CD, whereas the intensities of the main- and post-edges of *a*-CD are stronger. For *g*-CD, these three features are weaker than those of the other two CDs samples. The C=O feature of CDs around 532 eV can be slightly visible on transmission-XA spectra, while the other bands observed on TEY-XAS (Figure S2) are overlapped by the water signals. The contribution from C=O bonds from CDs appears enhanced on TIY-XA spectra compared to transmission measurements at similar concentration (Figure S2). Together with their clear contribution on TIY-XAS at the carbon K edge, this indicates that surface carboxyl groups act as a channel for electrons transfer between CDs and the surrounding water molecules.

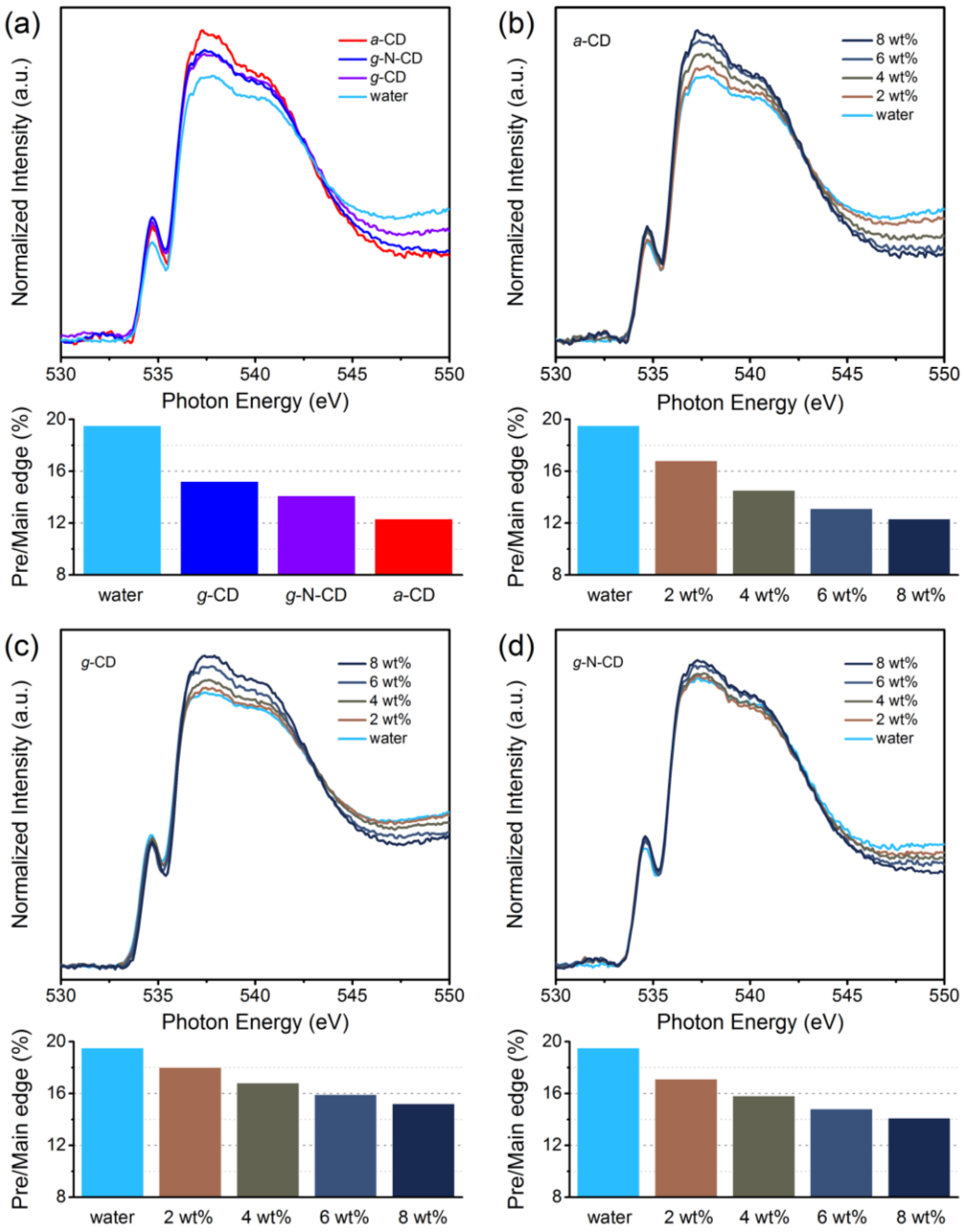

Figure 3. Transmission mode XA spectra at O K-edge from (a) water and different CDs dispersions (8 wt%) and (b) *a*-CD, (c) *g*-CD, (d) *g*-N-CD at different concentrations. The spectra are normalized to their integrated area. The pre/main-edge ratios for each spectrum are plotted below XA spectra.

The differences shown in the O K-edge XA spectra between aqueous CDs dispersions and pure water can be interpreted in terms of modification of the hydrogen bonding network of water molecules surrounding CDs. As investigated in previous XAS studies of bulk water,[33,34] the pre-edge feature originates from unsaturated or dangling hydrogen bonds observed in liquid phase. The main edge is also related to the population of molecules with unsaturated hydrogen bonds, while the post-edge region is associated with the fully saturated hydrogen bonding network. In bulk ice, the pre- and main-edges are weaker compared to liquid water since all hydrogen atoms in ice participate in hydrogen bonds, while the post-edge is stronger than that of water. The interfacial water layers around nanoparticles dispersed in an aqueous environment forms a partially saturated hydrogen bonding network, which can be considered as the mixture of liquid water and ice.

To compare the influence on the hydrogen bonding network of water molecules from the CDs samples, the pre/main-edge ratios were calculated from the fitted oxygen XA spectra (see Table S2 and Figure S4). The pre/main-edge ratio of pure water spectra remains constant as 19%. The pre/main-edge ratios at 8 wt% concentration of *a*-CD, *g*-N-CD and *g*-CD were decreased by 37%, 28% and 22%, respectively, compared to the same ratio in pure water (Figure 3a), which confirms the contributions of both bulk water and the interfacial water around CDs in the oxygen K-edge spectra. The distinctive results of the pre/main-edge ratio represent the different hydrogen bonding networks around CDs, which can be influenced by the concentration, the nanoparticles size and the surface chemistry of the CDs.

To confirm the strong impact of these three CDs on the water structure, the evolution of oxygen K-edge XA spectra at various concentrations was probed (Figure 3b-d). The absorption in the pre-, main- and post-edge regions enhances upon increasing the *a*-CD concentrations from 2 to 8

wt% (Figure 3b). The larger spectral change shown in the *a*-CD dispersion can be partially attributed to its larger sizes (6.8 ± 2.3 nm)[27] compared to the other CDs samples (3.1 − 3.6 nm).[7] The hydrogen bonding networks induced by nanodiamonds of similar size as *a*-CD have been previously determined to extended over several solvation shells.[24] Due to this arrangement, more bulk water molecules are involved in the formation of hydrogen bonds with the CDs, leading to the increased absorption of the pre-edge feature. This strong interaction between the *a*-CD and water molecules can also be confirmed by the pronounced C-O features shown in the in situ XA spectra at carbon K-edge (Figure 2a).

For *g*-CD, XA spectra exhibit a prominent increase at the main- and post-edges with increasing concentration, while the pre-edge feature is only slightly changed (Figure 3c). The quenching of the pre-edge feature may result from the small size of *g*-CD (3.6 ± 1.0 nm)[7], resulting in a higher amount of interfacial water, poorly contributing to the pre-edge. It should be noted that the *g*-CD samples were synthesized using the same precursor as *a*-CD, but at a higher calcination temperature to induce graphitization. The amorphous structures generally possess larger sizes with a non-uniform distribution than well-graphitized samples. For *g*-N-CD, the presence of nitrogen doping facilitates the emission of electrons and thus induces strong polarization of the CDs surface. Because the water molecule has a strong dipole moment, the surface polarization orients water molecules with oxygen sites pointing toward the CDs surface, leaving two hydrogen atoms available for the dual hydrogen bond motif. As such, our results suggest that a more structured long-range change of water organization (resembling amorphous ice) is formed around CDs with nitrogen doping. The changes of the hydrogen bonding network of the water molecules around the CDs induced by hydration may also be important for the effective charge transfer shown in *g*-N-CD as compared to *g*-CDs. From these spectroscopic studies, it appears

that Lewis basic carbon sites and structured interfacial water layer are generated by the graphitization and nitrogen doping of the CDs core. Together with the enhanced light absorption and the facilitated electrons transfer, *g*-N-CD exhibits superiority to enhance photocatalytic hydrogen evolution by acting as conductive channels, efficiently separating the photogenerated charge carriers.

In summary, we have demonstrated direct spectroscopic evidence of the impact of carbon core structure on the charge transfer and hydration properties of CDs dispersed in water. In particular, we evidenced that efficient charge transfer to water occurs upon excitation of C=C bonds from CDs with graphitized core but not from CDs with amorphous core. To this aim, we performed in situ XAS measurements at the C K-edge by detecting the ionic current in aqueous CDs dispersion generated upon X-ray irradiation. Distinctive electronic structures of CDs originated from their unique structural properties and chemical functionalities were confirmed by comparing XAS measured with ionic yield to transmission and electron yield detections. Furthermore, changes of water hydrogen bonding network around CDs, probed at the O K-edge, were also found to depend on the CDs core structure. Ionic yield detection of XAS is a promising new method to probe photoactive sites on dispersed nanoparticles with element- and site-selectivities that may facilitate the design of new photosensitizers and photocatalysts.

Supporting Information.

Experimental sections; O K-edge TEY-XA spectra of three CDs samples, and O K-edge TIY-XA spectra of *a*-CD, *g*-N-CD and water; N K-edge TEY-XA spectrum of *g*-N-CD; fitting details and deconvolutions of the C K-edge TEY-XA spectra and O K-edge transmission mode XA spectra of CDs samples (PDF)

Author Contributions

The manuscript was written through contributions of all authors. All authors have given approval to the final version of the manuscript.

The authors declare no competing financial interest.

ACKNOWLEDGMENT

This work was financially supported by Volkswagen foundation (Freigeist Fellowship No. 89592), the Christian Doppler Research Association (Austrian Federal Ministry for Digital and Economic Affairs, and National Foundation for Research, Technology and Development) and OMV. The authors acknowledge the kind support from the staff of BESSY II (Germany) and of UVSOR-III (Japan) synchrotron facilities.

REFERENCES

(1) Roy, S. C.; Varghese, O. K.; Paulose, M.; Grimes, C. A. Toward Solar Fuels: Photocatalytic Conversion of Carbon Dioxide to Hydrocarbons. *ACS Nano* **2010**, *4*, 1259–1278.

(2) Yang, M.-Q.; Gao, M.; Hong, M.; Ho, G. W. Visible-to-NIR Photon Harvesting: Progressive Engineering of Catalysts for Solar-Powered Environmental Purification and Fuel Production. *Adv. Mater.* **2018**, *30*, 1802894.

(3) Bai, S.; Jiang, W.; Li, Z.; Xiong, Y. Surface and Interface Engineering in Photocatalysis. *ChemNanoMat* **2015**, *1*, 223–239.

(4) Hutton, G. A. M.; Martindale, B. C. M.; Reisner, E. Carbon Dots as Photosensitisers for Solar-Driven Catalysis. *Chem. Soc. Rev.* **2017**, *46*, 6111–6123.

(5) Li, H.; Kang, Z.; Liu, Y.; Lee, S.-T. Carbon Nanodots: Synthesis, Properties and Applications. *J. Mater. Chem.* **2012**, *22*, 24230–24253.

(6) Yu, H.; Shi, R.; Zhao, Y.; Waterhouse, G. I. N.; Wu, L.-Z.; Tung, C.-H.; Zhang, T. Smart Utilization of Carbon Dots in Semiconductor Photocatalysis. *Adv. Mater.* **2016**, *28*, 9454–9477.

(7) Martindale, B. C. M.; Hutton, G. A. M.; Caputo, C. A.; Prantl, S.; Godin, R.; Durrant, J. R.; Reisner, E. Enhancing Light Absorption and Charge Transfer Efficiency in Carbon Dots through Graphitization and Core Nitrogen Doping. *Angew. Chemie* **2017**, *129*, 6559–6563.

(8) Stöhr, J. *NEXAFS Spectroscopy*; Springer-Verlag: New York: New York, 1992.

(9) Ren, J.; Weber, F.; Weigert, F.; Wang, Y.; Choudhury, S.; Xiao, J.; Lauermann, I.; Resch-Genger, U.; Bande, A.; Petit, T. Influence of Surface Chemistry on Optical{,} Chemical and Electronic Properties of Blue Luminescent Carbon Dots. *Nanoscale* **2019**, *11*, 2056–2064.

(10) Seidel, R.; Winter, B.; Bradforth, S. E. Valence Electronic Structure of Aqueous Solutions: Insights from Photoelectron Spectroscopy. *Annu. Rev. Phys. Chem.* **2016**, *67*, 283–305.

(11) Fransson, T.; Harada, Y.; Kosugi, N.; Besley, N. A.; Winter, B.; Rehr, J. J.; Pettersson, L. G. M.; Nilsson, A. X-Ray and Electron Spectroscopy of Water. *Chem. Rev.* **2016**, *116*, 7551–7569.

(12) Smith, J. W.; Saykally, R. J. Soft X-Ray Absorption Spectroscopy of Liquids and Solutions. *Chem. Rev.* **2017**, *117*, 13909–13934.

(13) Freiwald, M.; Cramm, S.; Eberhardt, W.; Eisebitt, S. Soft X-Ray Absorption Spectroscopy in Liquid Environments. *J. Electron Spectros. Relat. Phenomena* **2004**, *137–140*, 413–416.

(14) Nagasaka, M.; Hatsui, T.; Horigome, T.; Hamamura, Y.; Kosugi, N. Development of a Liquid Flow Cell to Measure Soft X-Ray Absorption in Transmission Mode: A Test for Liquid Water. *J. Electron Spectros. Relat. Phenomena* **2010**, *177*, 130–134.

(15) Schön, D.; Xiao, J.; Golnak, R.; Tesch, M. F.; Winter, B.; Velasco-Velez, J.-J.; Aziz, E. F. Introducing Ionic-Current Detection for X-Ray Absorption Spectroscopy in Liquid Cells. *J. Phys. Chem. Lett.* **2017**, *8*, 2087–2092.

(16) Petit, T.; Ren, J.; Choudhury, S.; Golnak, R.; Lalithambika, S. S. N.; Tesch, M. F.; Xiao, J.; Aziz, E. F. X-Ray Absorption Spectroscopy of TiO_2 Nanoparticles in Water Using a Holey Membrane-Based Flow Cell. *Adv. Mater. Interfaces* **2017**, *4*, 1700755.

(17) Schön, D.; Golnak, R.; Tesch, M. F.; Winter, B.; Velasco-Velez, J.-J.; Aziz, E. F.; Xiao, J. Bulk-Sensitive Detection of the Total Ion Yield for X-Ray Absorption Spectroscopy in

Liquid Cells. *J. Phys. Chem. Lett.* **2017**, *8*, 5136–5140.

(18) Cappa, C. D.; Smith, J. D.; Wilson, K. R.; Saykally, R. J. Revisiting the Total Ion Yield X-Ray Absorption Spectra of Liquid Water Microjets. *J. Phys. Condens. Matter* **2008**, *20*, 205105.

(19) Xi, L.; Schellenberger, M.; Präg, R. F.; Golnak, R.; Schuck, G.; Lange, K. M. Ionic Current Mn K-Edge X-Ray Absorption Spectra Obtained in a Flow Cell. *J. Phys. Chem. C* **2018**, *122*, 15588–15594.

(20) Wernet, P.; Nordlund, D.; Bergmann, U.; Cavalleri, M.; Odelius, M.; Ogasawara, H.; Näslund, L. Å.; Hirsch, T. K.; Ojamäe, L.; Glatzel, P.; *et al.* The Structure of the First Coordination Shell in Liquid Water. *Science (80-.).* **2004**, *304*, 995 LP-999.

(21) Smith, J. D.; Cappa, C. D.; Wilson, K. R.; Messer, B. M.; Cohen, R. C.; Saykally, R. J. Energetics of Hydrogen Bond Network Rearrangements in Liquid Water. *Science (80-.).* **2004**, *306*, 851 LP-853.

(22) Cappa, C. D.; Smith, J. D.; Wilson, K. R.; Messer, B. M.; Gilles, M. K.; Cohen, R. C.; Saykally, R. J. Effects of Alkali Metal Halide Salts on the Hydrogen Bond Network of Liquid Water. *J. Phys. Chem. B* **2005**, *109*, 7046–7052.

(23) Nagasaka, M.; Mochizuki, K.; Leloup, V.; Kosugi, N. Local Structures of Methanol–Water Binary Solutions Studied by Soft X-Ray Absorption Spectroscopy. *J. Phys. Chem. B* **2014**, *118*, 4388–4396.

(24) Petit, T.; Yuzawa, H.; Nagasaka, M.; Yamanoi, R.; Osawa, E.; Kosugi, N.; Aziz, E. F. Probing Interfacial Water on Nanodiamonds in Colloidal Dispersion. *J. Phys. Chem. Lett.* **2015**, *6*, 2909–2912.

(25) Petit, T.; Puskar, L.; Dolenko, T. A.; Choudhury, S.; Ritter, E.; Burikov, S.; Laptinskiy, K.; Brzustowski, Q.; Schade, U.; Yuzawa, H.; *et al.* Unusual Water Hydrogen Bond Network around Hydrogenated Nanodiamonds. *J. Phys. Chem. C* **2017**, *121*, 5185–5194.

(26) Ray, S. C.; Tsai, H. M.; Chiou, J. W.; Bose, B.; Jan, J. C.; Kumar, K.; Pong, W. F.; Dasgupta, D.; Tsai, M.-H. X-Ray Absorption Spectroscopy (XAS) Study of Dip Deposited a-C:H(OH) Thin Films. *J. Phys. Condens. Matter* **2004**, *16*, 5713.

(27) Martindale, B. C. M.; Hutton, G. A. M.; Caputo, C. A.; Reisner, E. Solar Hydrogen Production Using Carbon Quantum Dots and a Molecular Nickel Catalyst. *J. Am. Chem. Soc.* **2015**, *137*, 6018–6025.

(28) Weber, F.; Ren, J.; Petit, T.; Bande, A. Theoretical X-Ray Absorption Spectroscopy Database Analysis for Oxidised 2D Carbon Nanomaterials. *Phys. Chem. Chem. Phys.* **2019**, *21*, 6999–7008.

(29) Ding, W.; Wei, Z.; Chen, S.; Qi, X.; Yang, T.; Hu, J.; Wang, D.; Wan, L.-J.; Alvi, S. F.; Li, L. Space-Confinement-Induced Synthesis of Pyridinic- and Pyrrolic-Nitrogen-Doped Graphene for the Catalysis of Oxygen Reduction. *Angew. Chemie Int. Ed.* **2013**, *52*, 11755–11759.

(30) Guo, D.; Shibuya, R.; Akiba, C.; Saji, S.; Kondo, T.; Nakamura, J. Active Sites of Nitrogen-Doped Carbon Materials for Oxygen Reduction Reaction Clarified Using Model Catalysts. *Science (80-.).* **2016**, *351*, 361 LP-365.

(31) Bhattacharyya, S.; Ehrat, F.; Urban, P.; Teves, R.; Wyrwich, R.; Döblinger, M.; Feldmann, J.; Urban, A. S.; Stolarczyk, J. K. Effect of Nitrogen Atom Positioning on the Trade-off between Emissive and Photocatalytic Properties of Carbon Dots. *Nat. Commun.* **2017**, *8*, 1401.

(32) Meng, N.; Ren, J.; Liu, Y.; Huang, Y.; Petit, T.; Zhang, B. Engineering Oxygen-Containing and Amino Groups into Two-Dimensional Atomically-Thin Porous Polymeric Carbon Nitrogen for Enhanced Photocatalytic Hydrogen Production. *Energy Environ. Sci.* **2018**, *11*, 566–571.

(33) Tse, J. S.; Shaw, D. M.; Klug, D. D.; Patchkovskii, S.; Vankó, G.; Monaco, G.; Krisch, M. X-Ray Raman Spectroscopic Study of Water in the Condensed Phases. *Phys. Rev. Lett.* **2008**, *100*, 95502.

(34) Nilsson, A.; Nordlund, D.; Waluyo, I.; Huang, N.; Ogasawara, H.; Kaya, S.; Bergmann, U.; Näslund, L.-Å.; Öström, H.; Wernet, P.; *et al.* X-Ray Absorption Spectroscopy and X-Ray Raman Scattering of Water and Ice; an Experimental View. *J. Electron Spectros. Relat. Phenomena* **2010**, *177*, 99–129.